Journal of Sound and Vibration (2000) **232**(4), 823–833
doi:10.1006/jsvi.1999.2763, available online at http://www.idealibrary.com on IDEAL®

LETTERS TO THE EDITOR

A SIMPLE METHOD FOR THE ANALYSIS OF DEEP CAVITY AND LONG NECK ACOUSTIC RESONATORS

A. Doria

Università degli studi di Padova, Dipartimento di Ingegneria Meccanica, Via Venezia 1, 35131 *Padova, Italy*

(*Received* 26 *August* 1999, *and in final form* 26 *October* 1999)

1. INTRODUCTION

Acoustic resonators are used for controlling acoustic vibrations in several machines such as jet engines, rocket combustors, industrial furnaces, automobile engines and refrigerator compressors [1, 2]. Moreover, the acoustic study of intake manifolds of internal combustion engines is frequently carried out by means of a lumped element approach, in which Helmholtz resonators represent single-cylinder engines, whereas multiple resonators represent multi-cylinder engines [3, 4].

The basic physics of acoustic resonators have been well known for many years [5]. In most cases the natural frequency and transmission loss (TL) of resonators are calculated by using a lumped element model that holds when any characteristic dimension of the resonator is much smaller than the wavelength. Since the lumped element model only depends on the volume of the cavity, the area and length of orifice [6], it does not give any information about the influence of the other geometrical properties of the resonator (e.g., the area and length of the cavity) on the acoustic behaviour of the device.

In recent years, several researchers have carried out interesting studies in order to overcome the limitations of the lumped element approach and to take into account the details of resonator geometry.

Chanaud [7, 8] following the approach of Rayleigh and others, proposed improved formulas for calculating end corrections. His results showed the influence of orifice location and that the natural frequency differs significantly from the value calculated by using the lumped element model both when the cavity is deep and when the cavity is very wide (pancake resonator). These effects may be caused by the presence of the longitudinal and cross-modes of the cavity.

Selamet *et al.* [9] considered a series of concentric, cylindrical Helmholtz resonators having a fixed volume and different cavity length-to-diameter ratios. The natural frequencies and the transmission losses were evaluated experimentally and were compared with the results obtained from one-dimensional acoustic theory and with the results obtained from a one-dimensional finite difference numerical method. Good agreement between the experimental and the calculated results was found for length-to-diameter ratios greater than 1 (when the axial propagation is the most important).

In a later paper, Dickney and Selamet [10] studied resonators having small cavity length-to-diameter ratios and pointed out the effect of radial propagation on the natural frequency and transmission loss.

The recent introduction of self-tuning resonators [11], which are equipped with variable volumes or variable ducts, increases the interest in determining resonator natural frequencies with accuracy.

0022-460X/00/190823 + 11 $35.00/0

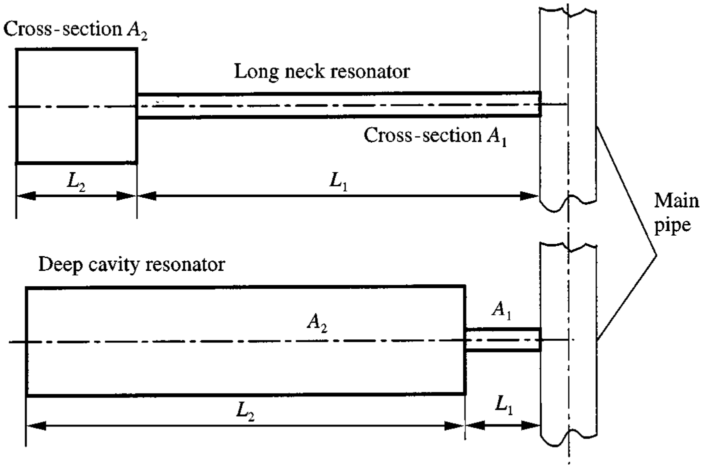

Figure 1. Deep cavity and long neck resonators.

In this paper, deep cavity and long neck resonators are considered where one of the axial lengths is not significantly smaller than the sound wavelength (see Figure 1). The axial motion of the fluid inside a deep cavity and the non-uniform motion of the fluid along a long neck are taken into account by means of linear or quadratic shape functions. In other words, the deep cavity or the long neck are represented by a simple one-dimensional finite element.

Mathematical models of resonators having few degrees of freedom (d.o.f.) are developed and analytical expressions of the natural frequencies and impedances are derived. Calculated results are compared with predictions from one-dimensional acoustic theory and with experimental results.

2. MATHEMATICAL MODEL

The mathematical model is developed according to the Lagrange approach and the generalized co-ordinates represent the displacements of the fluid in several sections of the neck and of the cavity.

The element of the resonator that is much smaller than the sound wavelength is modelled by following the lumped element approach. A short neck has kinetic energy

$$E_{ki} = \tfrac{1}{2}\rho A_i L_i \dot{x}_i^2, \tag{1}$$

where ρ is the density, A_i the cross-section, L_i the length and $\dot{x}_i$ the fluid velocity inside the neck. A short cavity, on the other hand, has potential energy

$$E_{pi} = \frac{1}{2}\frac{\rho c^2}{V_i} A_{i-1}^2 x_{i-1}^2, \tag{2}$$

where c is the sound speed, V_i the volume, A_{i-1} the neck cross-section and x_{i-1} the fluid displacement at the outlet of the neck.

Both the inertia and the compressibility of the fluid are taken into account in the longer element (deep cavity or long neck). The actual one-dimensional fluid motion is approximated by means of shape functions. If a linear shape function is used, the displacement of the fluid (u) in a generic section of the element depends, in a linear way, on the displacement at the inlet of the element (x_i) and the displacement at the outlet of the element (x_{i+1}):

$$u = \tfrac{1}{2}(1 - r)x_i + \tfrac{1}{2}(1 + r)x_{i+1}, \quad -1 \leqslant r \leqslant 1. \tag{3}$$

The kinetic and potential energies of the element are calculated according to the equations [13]

$$E_{ki} = \frac{1}{2}\int_{V_i} \rho \dot{u}^2 \, \mathrm{d}V, \qquad E_{pi} = \frac{1}{2}\int_{V_i} \rho c^2 \left(\frac{\mathrm{d}u}{\mathrm{d}x}\right)^2 \mathrm{d}V, \tag{4, 5}$$

resulting in

$$E_{ki} = \frac{1}{6}\rho A_i L_i(\dot{x}_i^2 + \dot{x}_{i+1}^2 + \dot{x}_i\dot{x}_{i+1}), \qquad E_{pi} = \frac{1}{2}\frac{A_i}{L_i}\rho c^2(x_i - x_{i+1})^2. \tag{6, 7}$$

If a quadratic shape function is used, the displacement of the fluid in a generic section of an element depends, in a quadratic way, on the displacements at the inlet (x_i), the middle (x_{i+1}) and the outlet of the element (x_{i+2}):

$$u = \tfrac{1}{2}r(r - 1)x_i + (1 - r^2)x_{i+1} + \tfrac{1}{2}r(r + 1)x_{i+2}, \quad -1 \leqslant r \leqslant 1. \tag{8}$$

The resulting kinetic and potential energies are

$$E_{ki} = \frac{1}{30}\rho A_i L_i(2\dot{x}_i^2 + 8\dot{x}_{i+1}^2 + 2\dot{x}_{i+2}^2 + 2\dot{x}_{i+1}\dot{x}_{i+2} + 2\dot{x}_{i+1}\dot{x}_i - \dot{x}_{i+2}\dot{x}_i), \tag{9}$$

$$E_{pi} = \frac{1}{6}\frac{A_i}{L_i}\rho c^2(7x_i^2 + 16x_{1+1}^2 + 7x_{i+2}^2 - 16x_{i+1}x_{i+2} - 16x_i x_{i+1} + 2x_i x_{i+2}). \tag{10}$$

The length of the neck is corrected with account taken of radiation-mass loading at the inlet and outlet of the neck [12]: the correction is $0.6a$ if the end is unflanged and $0.85a$ if the end is flanged, where a is the radius of the neck.

The total kinetic and potential energies of the resonators represented in Figure 1 are calculated by adding the term of the shorter element and the terms of longer element. Then the continuity equation is used to correlate the velocity at the outlet of the neck ($\dot{x}_n$) with the velocity at the inlet of the cavity ($\dot{x}_c$):

$$\dot{x}_c A_2 = \dot{x}_n A_1. \tag{11}$$

Since the initial displacements are assumed to be zero, if the continuity equation is integrated, the following equation holds:

$$x_c A_2 = x_n A_1. \tag{12}$$

The acoustic equations are derived by using the Lagrange method and have the form

$$[\mathbf{M}]\{\ddot{x}\} + [\mathbf{K}]\{x\} = \{\mathbf{F}\}, \tag{13}$$

where $[\mathbf{M}]$ is the mass matrix, $[\mathbf{K}]$ the stiffness matrix, $\{x\}$ the displacement vector and $\{\ddot{x}\}$ the acceleration vector. $\{\mathbf{F}\}$ is the generalized forces vector; it contains a non-zero term which depends on pressure $p(t)$ at the inlet of the neck.

The proposed method, like the classical one-dimensional acoustic theory, is well suited for studying the steady state response of the acoustic system to a harmonic input. Moreover, since the resonator is modelled as a simple multi-degree-of-freedom vibrating system, the time-domain response of the resonator to a generic pressure input can be calculated with standard techniques and in many cases an analytical solution is possible. This kind of analysis is of particular interest in the field of engine simulation [4].

In this paper, equation (13) was solved analytically in the presence of a harmonic pressure input $p(t) = p_0 \mathrm{e}^{\mathrm{i}\omega t}$ where p_0 is the pressure fluctuation amplitude and ω the angular frequency. Then the resonator impedance was calculated. The resonator impedance Z_r is the ratio between input pressure and volume velocity $\dot{x}_1 A_1$ entering the duct

$$Z_r = R_r + \mathrm{i}X_r = \frac{p_0 \mathrm{e}^{\mathrm{i}\omega t}}{\dot{x}_1 A_1}, \tag{14}$$

where R_r is the acoustic resistance and X_r the acoustic reactance. In the present model, which does not take energy dissipation into account, the resonator resistance is zero. The calculated formulas for the acoustic impedances of the resonators are presented in the following sections.

2.1. DEEP CAVITY RESONATOR

If a linear shape function is used to represent the fluid motion inside the cavity, the model has only one d.o.f. since the cavity is closed and the displacement of the fluid at the inlet of the cavity is related to the displacement in the neck according to the continuity equation. Therefore, the acoustic equation is

$$\frac{1}{3}\frac{(A_1 L_2 + 3A_2 L_1)\rho A_1}{A_2}\ddot{x}_1 + \frac{\rho A_1^2 c^2}{A_2 L_2} x_1 = p(t) A_1, \tag{15}$$

and the resonator reactance is

$$X_r = -\frac{1}{3}\frac{(3c^2 A_1 - (A_1 L_2 + 3A_2 L_1)\omega^2 L_2)\rho}{\omega A_2 A_1 L_2}. \tag{16}$$

The frequency equation is given when the reactance is made equal to zero; the first natural frequency is

$$\omega_1 = \sqrt{3\,\frac{c^2 A_1}{(A_1 L_2 + 3A_2 L_1) L_2}}. \tag{17}$$

If a quadratic shape function is used, the model of the resonator has two d.o.f. and the first two natural frequencies are predicted. The generalized co-ordinates are the displacements of the fluid in the neck and middle of the cavity. The mass and stiffness matrices can be found in Appendix A. The resonator reactance is

$$X_r = -\frac{1}{24}\,\frac{\rho(3(A_1L_2 + 8A_2L_1)\omega^4L_2^3 - 8c^2(13A_1L_2 + 30A_2L_1)\omega^2L_2 + 240c^4A_1)}{A_2A_1L_2(-L_2^2\omega^2 + 10c^2)\omega}. \qquad (18)$$

The frequency equation is obtained when the reactance is made equal to zero. It is a standard biquadratic equation having analytical solutions that make it easier to carry out a parametric analysis of resonator behaviour.

2.2. LONG NECK RESONATOR

When a linear shape function is used to represent the non-uniform fluid motion inside the neck, the model has two d.o.f. The generalized co-ordinates are the displacement at the inlet and outlet of the neck. The resonator reactance is given by

$$X_r = -\frac{1}{4}\,\frac{\rho(A_2L_2L_1^3\omega^4 - 4(3A_2L_2 + A_1L_1)L_1c^2\omega^2 + 12A_1c^4)}{A_1(-A_2L_2L_1^2\omega^2 + 3A_2L_2c^2 + 3A_1L_1c^2)\omega}. \qquad (19)$$

The frequency equation is a standard biquadratic equation and has analytical solutions, which are the first two natural frequencies of the resonator.

If the non uniform motion of the fluid inside the neck is represented by a parabolic shape function, the resonator model has three d.o.f. and three natural frequencies can be predicted. The third generalized co-ordinate is the fluid displacement at the middle of the neck. The resonator reactance is given by

$$X_r = -\frac{1}{3} \times \frac{\rho(-A_2L_2L_1^5\omega^6 + 9(8A_2L_2 + A_1L_1)L_1^3c^2\omega^4 - 24(30A_2L_2 + 13A_1L_1)L_1c^4\omega^2 + 720A_1c^6)}{A_1(3A_2L_2L_1^4\omega^4 + (-24A_1L_1^3c^2 - 104A_2L_2L_1^2c^2)\omega^2 + 240(A_2L_2 + A_1L_1)c^4)\omega}. \qquad (20)$$

In this case, the frequency equation, which is a third order algebraic equation in ω^2, can be solved numerically.

3. COMPARISON WITH THE CLASSICAL ONE-DIMENSIONAL ACOUSTIC THEORY

The transmission (TL) loss for a Helmholtz resonator attached to an infinitely long pipe with no mean flow is given by [12, 13]

$$TL = 10\log_{10}\frac{((\rho c/2S) + R_r)^2 + X_r^2}{R_r^2 + X_r^2}, \qquad (21)$$

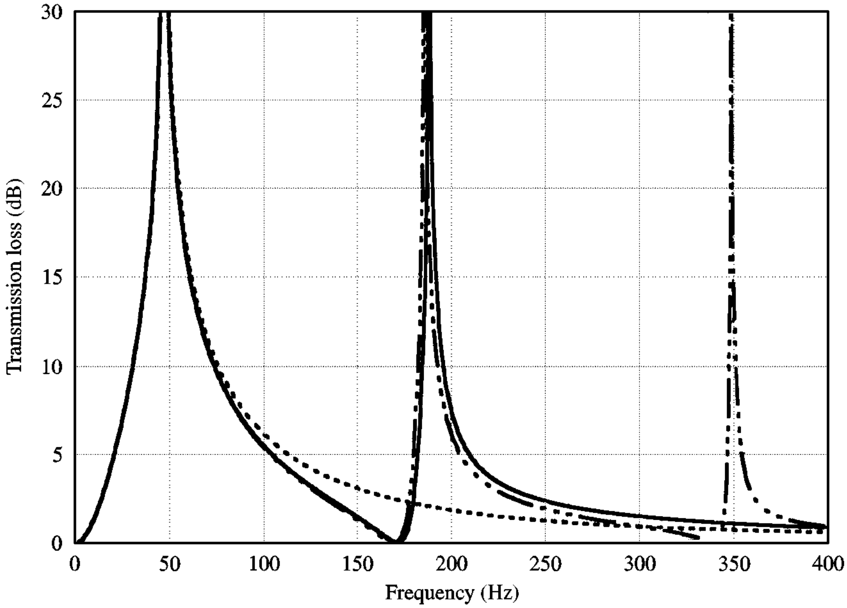

Figure 2. Transmission loss of the deep cavity resonator; comparison with one-dimensional acoustics results: ——- - - -—, equation (22); - - - -, linear; ——, parabolic.

where S is the pipe cross-section. If R_r is assumed to be zero, the classical acoustic theory gives the following expression for the transmission loss [9]:

$$TL = 10\log_{10}\left(1 + \left(\frac{A_1}{2S}\,\frac{\tan(kL_1) + (A_2/A_1)\tan(kL_2)}{1 - (A_2/A_1)\tan(kL_2)\tan(kL_1)}\right)^2\right), \tag{22}$$

where $k = \omega/c$.

The transmission losses of the deep cavity and long neck resonators can also be calculated by means of the proposed method, if the values of the acoustic reactances presented in Sections 2.1 and 2.2 are put into equation (21).

Figure 2 deals with a deep cavity resonator; the cavity is 1 m long and has a square cross-section ($0{\cdot}1 \times 0{\cdot}1$ m), the neck has radius $a = 0{\cdot}016$ and is 0·05 m long. The TL predicted by the model, which is based on a linear shape function, is in good agreement with the TL given by equation (22) as long as the forcing frequency is lower than the second natural frequency. If the parabolic shape function is used, the agreement is good as long as the forcing frequency is lower than the third natural frequency.

Figure 3 deals with a long neck resonator, the cavity is cube shaped (side 0·1 m), the neck has radius $a = 0{\cdot}016$ m and is 1 m long. In this case there is good agreement between the TL given by the different methods as long as the forcing frequency is lower than the second natural frequency. When the forcing frequency is higher, the agreement is not as good, because the two methods which are based on shape functions predict a value of the second natural frequency that is 13% higher than the one predicted by the classical one-dimensional acoustic theory.

4. EXPERIMENTAL APPARATUS

In order to compare the results given by the proposed method with experimental results, an adjustable resonator was built. The cavity of the resonator has a square cross-section

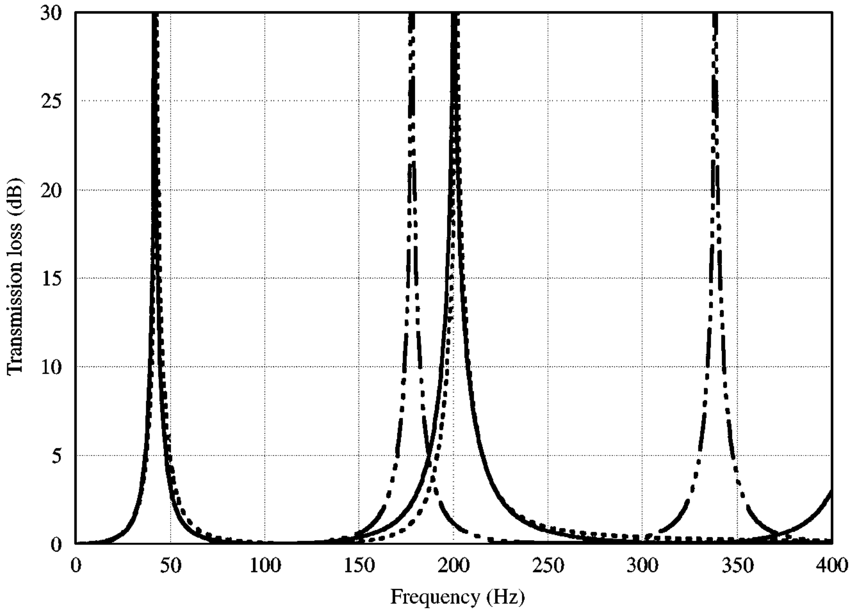

Figure 3. Transmission loss of the long neck resonator; comparison with one-dimensional acoustics results: —---—, equation (22); ----, linear; ——, parabolic.

(0·1 × 0·1 m) and an adjustable depth (minimum depth 0·02 m, maximum depth 1 m). The resonator neck is made up of modular elements having circular cross-sections ($a = 0{\cdot}016$ m): the shortest element is 0·01 m long and when all the elements are mounted, the neck is 1·2 m long. There is no baffle at the end of the neck. All resonator elements are made of Plexiglass.

The resonator's natural frequencies are measured by using two microphones, a loudspeaker driven by a wave generator and a Fourier analyzer; the experimental method is similar to the one proposed by Chanaud [8].

The resonator and the loudspeaker are placed in a reasonably sound absorptive room. One microphone measures the sound pressure inside the resonator cavity and is inserted in the wall opposite to the neck; the other microphone measures the sound pressure outside of the resonator. The loudspeaker (driven by the wave generator) produces pure tones of increasing frequency with a step of 0·25 Hz. A natural frequency is identified when the sound pressure measured inside the resonator cavity is much larger than the sound pressure measured outside the resonator.

5. COMPARISON WITH EXPERIMENTAL RESULTS

In the first test the effect of cavity depth was considered and the length of the neck was kept constant (0·05 m). The first natural frequency calculated by means of the proposed method was compared to the experimental value and to the value calculated according to the classical lumped element method [12] by using the equation

$$f = \frac{c}{2\pi}\sqrt{\frac{A_1}{(L_1 + 1{\cdot}45a)V_2}}, \tag{23}$$

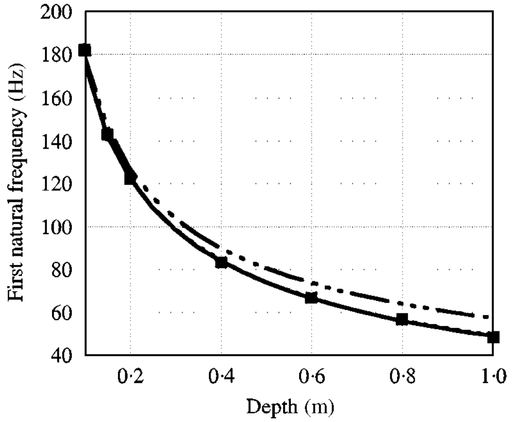

Figure 4. First natural frequency of the deep cavity resonator; comparison with experimental results: ■, experimental; - - - -, linear; ——, parabolic; — - - - —, equation (23).

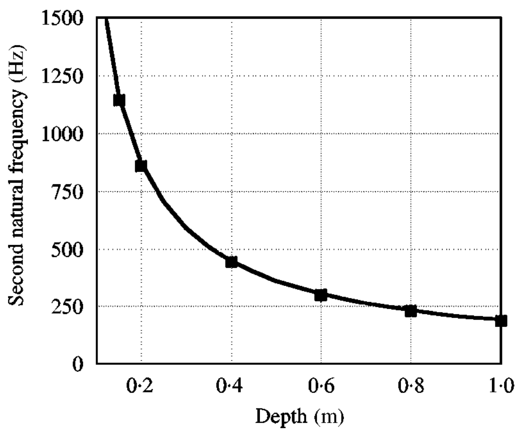

Figure 5. Second natural frequency of the deep cavity resonator; comparison with experimental results: ■, experimental; ——, parabolic.

where the duct length is corrected with the inlet considered unflanged and the outlet flanged.

Figure 4 shows that the first natural frequency decreases when the cavity depth increases. The lumped element equation (23) overestimates the first natural frequency (maximum error 18%). The model that is based on a linear shape function (one d.o.f. model) and the model that is based on a parabolic shape function (two d.o.f. model) predict essentially the same frequency. The agreement with experimental results is very good for all the values of cavity depth and the maximum error (3%) takes place when the volume is cube shaped ($L_2 = 0{\cdot}1$ m). When $L_2 = 1$ m, the first natural frequency is 48·25 Hz and the corresponding wavelength (λ) is about 7 m; hence, the effect of cavity length is important when $L_2/\lambda > 1/10$.

The two d.o.f. model makes it possible to predict the second natural frequency of the resonator. Figure 5 shows that the second natural frequency also decreases with the cavity depth and that the proposed method estimates this frequency with good accuracy (maximum error $\approx 2\%$).

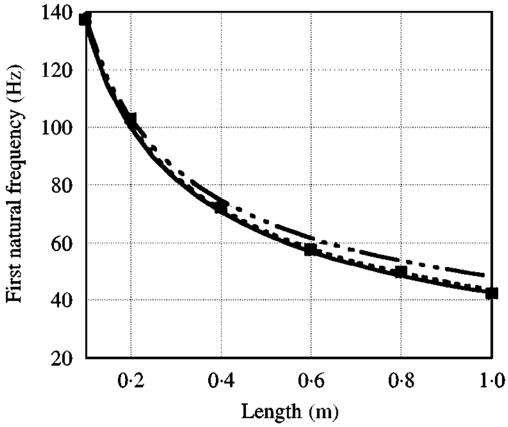

Figure 6. First natural frequency of the long neck resonator; comparison with experimental results: ■, experimental; - - - -, linear; ——, parabolic; —- - - -— equation (23).

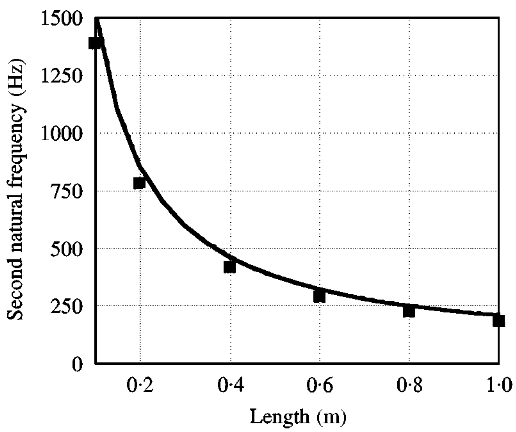

Figure 7. Second natural frequency of the long neck resonator; comparison with experimental results: ■, experimental; - - - -, linear; ——, parabolic.

In the second test, the neck length was varied in the range 0·1–1 m and the cavity volume was kept constant (cube-shaped cavity with the side 0·1 m long). Figure 6 shows that the lumped element equation (23) overestimates the first natural frequency, which decreases when the neck length increases; with $L_1 = 1$ m the error is about 13%. The proposed method, which models the fluid motion inside the neck by means of shape functions, shows smaller errors when neck length increases; the error is less than 2% when the neck is long. It is interesting to highlight that, when $L_1 = 1$ m, the first natural frequency is 42·5 Hz and the corresponding wavelength (λ) is about 8 m; hence, the effect of non uniform velocity distribution along the neck is already important when $L_1/\lambda > 1/10$.

The second natural frequency may be calculated by using both the two d.o.f. model (linear shape function) and the three d.o.f. model (parabolic shape function). Figure 7 shows the comparison between the calculated values and the experimental values, in this case the error is about 12% both when the duct is short and when the duct is long.

6. CONCLUSIONS

Deep cavity and long neck resonators can be modelled as simple multi-degree-of-freedom vibrating systems if the fluid motion inside the longer element is simulated by means of a shape function.

The calculated reactances are ratios between polynomials; hence, the frequency equations are simple algebraic equations, whereas the classical one-dimensional acoustic theory leads to trigonometric frequency equations.

The comparison with experimental results showed that both the model based on a linear shape function and the one based on a parabolic shape function predicted the first natural frequency of the resonator with good accuracy. The models with two or more d.o.f. also gave a good estimate of the second natural frequency of the resonator.

ACKNOWLEDGMENT

The author is grateful to Professor V. Cossalter for his advice and to the graduating student A. Cattaneo for the collaboration in the construction of the resonator.

APPENDIX A

Matrices of the deep cavity resonator, two d.o.f. model:

$$[\mathbf{M}] = \rho\,\frac{1}{15}\begin{bmatrix} \dfrac{(2A_1L_2 + 15A_2L_1)A_1}{A_2} & A_1L_2 \\ A_1L_2 & 8A_2L_2 \end{bmatrix}, \quad [\mathbf{K}] = \frac{1}{3}\,\frac{\rho c^2}{L_2}\begin{bmatrix} 7\dfrac{A_1^2}{A_2} & -8A_1 \\ -8A_1 & 16A_2 \end{bmatrix}$$

Matrices of the long neck resonator, two d.o.f. model:

$$[\mathbf{M}] = \frac{1}{3}\,\rho A_1L_1\begin{bmatrix} 1 & \frac{1}{2} \\ \frac{1}{2} & 1 \end{bmatrix}, \quad [\mathbf{K}] = \frac{\rho c^2A_1}{L_1}\begin{bmatrix} 1 & -1 \\ -1 & \dfrac{(A_2L_2 + A_1L_1)}{A_2L_2} \end{bmatrix}.$$

Matrices of the long neck resonator, three d.o.f. model:

$$[\mathbf{M}] = \frac{1}{15}\,\rho A_1L_1\begin{bmatrix} 2 & 1 & -\frac{1}{2} \\ 1 & 8 & 1 \\ -\frac{1}{2} & 1 & 2 \end{bmatrix}, \quad [\mathbf{K}] = \frac{1}{3}\,\frac{\rho c^2A_1}{L_1}\begin{bmatrix} 7 & -8 & 1 \\ -8 & 16 & -8 \\ 1 & -8 & \dfrac{[7A_2L_2 + 3A_1L_1]}{A_2L_2} \end{bmatrix}.$$

REFERENCES

1. P. K. TANG and W. A. SIRIGNANO 1973 *Journal of Sound and Vibration* **26**, 247–262. Theory of a generalized Helmholtz resonator.
2. V. COSSALTER, A. DORIA and F. GIUSTO 1994 *Proceedings of the* 1994 *International Compressor Engineering Conference at Purdue*, Vol. 2, 563–568. Control of acoustic vibration inside refrigerator compressors by means of resonators: comparison between analytical and experimental results.

3. H. W. Engelman 1973 *ASME Paper Series*, *paper* 73-*WA*/*DGP*-2. Design of a tuned intake manifold.
4. D. Bortoluzzi, V. Cossalter and A. Doria 1998 *Proceedings* 1998 *Motorsports Engineering Conference*, Vol. 2, 79–87 (*SAE* 983045). The effect of tunable resonators on the volumetric efficiency of an engine.
5. Lord Rayleigh (J. W. S. STRUTT) 1964 *Scientific Papers*, Vol. 1. New York: Dover.
6. A. Doria 1995 *Journal of Sound and Vibration* **181**, 673–685. Control of acoustic vibrations of an enclosure by means of multiple resonators.
7. R. C. Chanaud 1994 *Journal of Sound and Vibration* **178**, 337–348. Effects of geometry on the resonance frequency of Helmholtz resonators.
8. R. C. Chanaud 1997 *Journal of Sound and Vibration* **204**, 829–834. Effects of geometry on the resonance frequency of Helmholtz resonators, Part II.
9. A. Selamet, N. S. Dickey and J. M. Novak 1995 *Journal of Sound and Vibration* **187**, 358–367. Theoretical, computational and experimental investigation on Helmholtz resonators with fixed volume: lumped versus distributed analysis.
10. N. S. Dickey and A. Selamet 1996 *Journal of Sound and Vibration* **195**, 512–517. Helmholtz resonators: one-dimensional limit for small cavity length-to-diameter ratios.
11. J. M. De Bedout, M. A. Franchek, R. J. Bernhard and L. Mongeau 1997 *Journal of Sound and Vibration* **202**, 109–123. Adaptive-passive noise control with self-tuning Helmholtz resonators.
12. L. Kinsler, A. Frey, A. Coppens and J. Sanders 1982 *Fundamental of Acoustics*. New York: John Wiley, third edition.
13. M. L. Munjal 1987 *Acoustics of Ducts and Mufflers*. New York: John Wiley.